Role of Multidrug Resistance–Associated Protein 4 in the Basolateral Efflux of Hepatically Derived Enalaprilat

Brian C. Ferslew,[1] Kathleen Köck,[2] Arlene S. Bridges, and Kim L. R. Brouwer

Division of Pharmacotherapy and Experimental Therapeutics, UNC Eshelman School of Pharmacy (B.C.F., K.K., K.L.R.B.) and Department of Pathology, UNC School of Medicine (A.S.B.), University of North Carolina at Chapel Hill, Chapel Hill, North Carolina

ABSTRACT

Hepatic uptake and efflux transporters govern the systemic and hepatic exposure of many drugs and metabolites. Enalapril is a pharmacologically inactive prodrug of enalaprilat. Following oral administration, enalapril is converted to enalaprilat in hepatocytes and undergoes translocation into the systemic circulation to exert its pharmacologic effect by inhibiting angiotensin-converting enzyme. Although the transport proteins governing hepatic uptake of enalapril and the biliary excretion of enalapril and enalaprilat are well established, it remains unknown how hepatically derived enalaprilat translocates across the basolateral membrane into the systemic circulation. In this study, the role of ATP-binding cassette transporters in the hepatic basolateral efflux of enalaprilat was investigated using membrane vesicles. ATP-dependent uptake of enalaprilat into vesicles expressing multidrug resistance–associated protein (MRP) 4 was significantly greater (~3.8-fold) than in control vesicles. In contrast, enalaprilat was not transported to a significant extent by MRP3, and enalapril was not transported by either MRP3 or MRP4. The functional importance of MRP4 in the basolateral excretion of derived enalaprilat was evaluated using a novel basolateral efflux protocol developed in human sandwich-cultured hepatocytes. Under normal culture conditions, the mean intrinsic basolateral efflux clearance ($CL_{int,basolateral}$) of enalaprilat was 0.026 ± 0.012 μl/min; enalaprilat $CL_{int,basolateral}$ was significantly reduced to 0.009 ± 0.009 μl/min by pretreatment with the pan-MRP inhibitor MK-571. Results suggest that hepatically derived enalaprilat is excreted across the hepatic basolateral membrane by MRP4. Changes in MRP4-mediated basolateral efflux may alter the systemic concentrations of this active metabolite, and potentially the efficacy of enalapril.

Introduction

The liver plays a central role in the metabolism, detoxification, and elimination of endogenous and exogenous compounds. Following uptake across the basolateral membrane from the blood to the hepatocyte, metabolism typically results in formation of a more hydrophilic, charged molecule that can be eliminated either via the bile or across the basolateral membrane into the systemic circulation for renal excretion. Importantly, following hydrophilic transformation, active efflux processes typically are required for the metabolite to exit the liver. In contrast to biliary excretion, changes in active basolateral efflux processes (either due to drug-drug interactions or disease-mediated changes in efflux transporter function) are underappreciated (Köck and Brouwer, 2012; Konig et al., 2013; Pfeifer et al., 2014). Changes in basolateral efflux of active metabolites may alter systemic concentrations and, thus, systemic efficacy/toxicity, and potentially warrant detailed evaluation during drug development (Köck and Brouwer, 2012; Zamek-Gliszczynski et al., 2014).

Enalapril is a prodrug transformed in the liver by carboxylesterases to the active moiety, enalaprilat. Transformation removes the ethylester from enalapril, adding a negative charge and increasing the potency to inhibit angiotensin-converting enzyme, thereby lowering blood pressure and preventing cardiac remodeling and renal dysfunction (Patchett et al., 1980). Due to the inherent negative charge on the parent drug and added polarity after metabolism, enalapril and enalaprilat require active transport processes to cross membranes. Interestingly, the presence of a diffusional barrier for enalapril and enalaprilat disposition helped lay the foundation for the identification of transporter-mediated disposition and clearance mechanisms of charged molecules (Pang et al., 1984, 1998; de Lannoy and Pang, 1986; Schwab et al., 1990). Rat organic anion transporting polypeptide (OATP) 1a1 and human OATP1B1 are responsible for the uptake of enalapril into the hepatocyte.

Enalaprilat derived in the liver can be excreted into the bile or translocated across the basolateral membrane into the systemic circulation (de Lannoy et al., 1993; Pang et al., 1998; Liu et al., 2006). Although multidrug resistance–associated protein (MRP) 2 is capable of excreting enalaprilat from the hepatocyte into bile, the majority of the absorbed dose of enalapril is excreted in the urine as enalaprilat, which suggests that basolateral efflux of enalaprilat into the systemic

ABBREVIATIONS: AUC, area under the curve; BEI, biliary excretion index; $CL_{biliary}$, biliary clearance; $CL_{int,basolateral}$, intrinsic basolateral efflux clearance; HBSS, Hanks' balanced salt solution; HEK, human embryonic kidney; LC-MS/MS, liquid chromatography–tandem mass spectrometry; Mrp/MRP, multidrug resistance–associated protein; Oatp/OATP, organic anion transporting polypeptide; SCH, sandwich-cultured hepatocytes; TSB, Tris-sucrose buffer; $X_{Efflux\ Buffer}$, cumulative amount of enalaprilat excreted from the cell over the efflux period.

circulation predominates since enalaprilat appears to be formed only in the hepatocyte (Tocco et al., 1982; Ulm et al., 1982; de Lannoy et al., 1993). As the site of action for enalaprilat is in the systemic circulation (inhibition of angiotensin-converting enzyme), hepatic basolateral efflux is germane in regulating enalaprilat's beneficial effects on blood pressure, cardiac remodeling, and kidney protection. Two proteins that may be able to transport enalaprilat from the hepatocyte into sinusoidal blood are MRP3 and MRP4. Substrate specificity profiles and the localization of MRP3 and MRP4 on the basolateral membrane make them prime candidates to mediate enalaprilat transport (Gradhand et al., 2008; Klaassen and Aleksunes, 2010; Chai et al., 2012).

Although enalapril is prescribed extensively in many chronic diseases, including diabetes, nonalcoholic fatty liver disease, and renal failure, little is known about how coadministered medications or disease-associated changes in MRP expression affect enalaprilat disposition. In addition to specific disease states, disease severity also can alter basolateral efflux transporter expression (Hardwick et al., 2011; Hanada et al., 2012; Tsujimoto et al., 2012; Köck et al., 2013; Yeung et al., 2014). For example, inflammation associated with nonalcoholic fatty liver disease increases protein expression of MRPs (e.g., MRP3, MRP4, MRP6) on the basolateral membrane (Hardwick et al., 2011). Without knowledge of the basolateral transport process(es) involved in enalaprilat disposition, it is difficult to accurately predict how disease state alterations and drug-drug interactions may impact systemic concentrations and pharmacological effects.

This study was designed to determine whether MRP3 and/or MRP4 is involved in the hepatic basolateral efflux of enalaprilat, and to demonstrate the impact of MRP inhibition on the hepatic basolateral efflux clearance of enalaprilat. Enalapril and enalaprilat transport were evaluated in membrane vesicles prepared from cells expressing either MRP3 or MRP4. Additionally, a novel experimental protocol was developed in human sandwich-cultured hepatocytes (SCH) to assess the potential impact of coadministered medications on enalaprilat basolateral efflux.

Materials and Methods

Enalapril maleate, d_5-enalapril, enalaprilat, d_5-enalaprilat, taurocholate, Hanks' balanced salt solution (HBSS), and Ca^{2+}/Mg^{2+}-free HBSS (Ca^{2+}-free HBSS) were purchased from Sigma-Aldrich (St. Louis, MO). MK-571 was purchased from Cayman Chemical Company (Ann Arbor, MI). Rosuvastatin was purchased from Toronto Research Chemicals (Toronto, Ontario, Canada). [^{3}H]Taurocholate (1 mCi/ml; >97% purity) and [^{3}H]rosuvastatin (1 mCi/ml; >97% purity) were purchased from PerkinElmer (Waltham, MA) and American Radiolabeled Chemicals (St. Louis, MO), respectively. All other chemicals were commercially available and of the highest grade available.

Human Embryonic Kidney Cell Culture and Overexpression of MRP3 and MRP4. Human MRP3 plasmid [pcDNA3.1(−)-MRP3] and MRP4 plasmid [pcDNA3.1(+)-MRP4] were kindly provided by Dr. Susan Cole (Queen's University, Kingston, Canada) and Dr. Dietrich Keppler (German Cancer Research Center, Heidelberg, Germany), respectively. Human embryonic kidney (HEK) 293T cells were cultured in Dulbecco's modified Eagle's medium supplemented with 10% fetal bovine serum in a humidified incubator.

For MRP4, a stable transfected cell line was developed as previously described (Köck et al., 2013). For MRP3, transient transfection of HEK293T cells with X-tremeGENE 9 DNA Transfection Reagent (Roche Diagnostics, Mannheim, Germany) was performed according to the manufacturer's instructions. Seventy-two hours after transfection, the cells were harvested. Nontransfected and control mock-transfected cells were used to generate control membrane vesicles for the MRP3 and MRP4 assays, respectively. Cells were harvested by trypsinizing and centrifuging the transporter-overexpressing cells and the respective control cell lines. The cell pellets were washed in Tris-sucrose buffer (TSB; 250 mM sucrose/50 mM Tris, pH 7.4) containing 0.25 mM $CaCl_2$. The final cell pellet was overlaid with 10 ml TSB containing 0.25 mM $CaCl_2$ and protease inhibitors (complete Mini EDTA-free; Roche Diagnostics), snap-frozen in liquid nitrogen, and stored at −80°C.

Membrane Vesicle Preparation. Membrane vesicles were prepared for MRP4, MRP3, and respective controls as described previously (Ghibellini et al., 2008). In brief, frozen cell pellets were thawed, resuspended in TSB, and exploded by N_2 cavitation (300 psi, 5 minutes). After addition of EDTA (1 mM), the suspension was centrifuged (800 × g, 10 minutes, 4°C) and the supernatant was collected. The pellet was resuspended in TSB with 0.5 mM EDTA and centrifuged (800 × g, 10 minutes, 4°C). The resulting supernatants were overlaid over 35% (w/w) sucrose/50 mM Tris buffer in a high-speed centrifuge tube. After centrifugation (100,000 × g, 90 minutes, 4°C), the interphase was collected and added to a new high-speed centrifuge tube with 25 mM sucrose/50 mM Tris buffer. After additional centrifugation (100,000 × g, 45 minutes, 4°C), the pellet was resuspended in 1 ml TSB. The suspension was added to a high-speed centrifuge tube and centrifuged (100,000 × g, 20 minutes, 4°C). The supernatant was discarded and the pellet was resuspended in TSB. Subsequently, the suspension was homogenized using a 27-gauge needle (15 strokes). The membrane vesicle suspension was divided into aliquots, snap-frozen in liquid nitrogen, and stored at −80°C until use. Successful transfection was confirmed via Western blotting and transport of radiolabeled prototypic probes as described previously (Köck et al., 2013).

Membrane Vesicle Assay. Membrane vesicles (10 μg) were incubated at 37°C with enalapril or enalaprilat (100 μM) with and without MK-571 (50 μM) in TSB containing $MgCl_2$ (10 mM), creatine phosphate (10 mM), creatine kinase (100 μg/ml), and ATP (4 mM) in a final volume of 50 μl. Enalapril, enalaprilat, and MK-571 stock solutions were prepared in TSB or 100% dimethylsulfoxide with a resulting dimethylsulfoxide final concentration of less than 1% in the total incubation volume. ATP was replaced by AMP (4 mM) for control reactions. At least three separate experiments in triplicate were performed for all incubations, unless otherwise noted. After incubation for 5 minutes, the reactions were stopped by addition of 800 μl of ice-cold TSB and immediately filtered through glass fiber filters (Pall Life Sciences, Port Washington, NY) presoaked in 3 mM reduced glutathione/10 mM dithiothreitol in TSB overnight. Filters were washed three times with ice-cold TSB. Filters were air dried and dissolved in 1 ml of pure high-performance liquid chromatography methanol containing d_5-enalapril and d_5-enalaprilat for liquid chromatography–tandem mass spectrometry (LC-MS/MS) analysis. ATP-dependent uptake was calculated as the difference in uptake in the presence of AMP and ATP. MRP-dependent substrate transport was calculated by subtracting ATP-dependent uptake in control membrane vesicles from uptake in membrane vesicles prepared from MRP3- or MRP4-expressing cells.

Sandwich-Cultured Hepatocyte Isolation and Culture. Human hepatocytes from three donors were kindly provided by Life Technologies (Research Triangle Park, NC) and Triangle Research Laboratories (Research Triangle Park, NC), and cultured as previously described (Swift et al., 2010). Hepatocyte donors included three Caucasian men ranging in age from 20 to 48 years with a body mass index of 19–31 kg/m^2. In brief, freshly isolated human hepatocytes were seeded in six-well BioCoat plates (BD Biosciences, San Jose, CA) at a density of 1.5 × 10^6 cells/well. Hepatocytes were overlaid with Matrigel basement membrane matrix (BD Biosciences) and maintained as described previously (Swift et al., 2010).

Sandwich-Cultured Hepatocyte Uptake and Biliary Excretion Studies. Determination of the uptake and biliary excretion of probe substrates in human SCH has been described previously (Abe et al., 2009). Slight modifications were made to allow determination of enalapril and enalaprilat uptake, formation, and excretion. In brief, human SCH were washed twice with 2 ml of warm Ca^{2+}-containing standard HBSS (cells + bile) or Ca^{2+}-free HBSS (cells) and incubated with 1.5 ml of the same buffer for 10 minutes at 37°C containing either [^{3}H]taurocholate (1 μM; 100 nCi/ml), [^{3}H]rosuvastatin (1 μM; 100 nCi/ml), or enalapril (5 μM). After 10 minutes, cells were washed three times with ice-cold standard HBSS and lysed with either 0.5% Triton X-100 in phosphate-buffered saline (for [^{3}H]taurocholate and [^{3}H]rosuvastatin analysis) or pure high-performance liquid chromatography grade methanol containing internal standards (for enalapril and enalaprilat analysis). Radioactivity in cell lysates was quantified by liquid scintillation spectroscopy (Packard Tri-Carb; PerkinElmer). Enalapril and enalaprilat were quantified in cell lysates using LC-MS/MS. Accumulation of taurocholate, rosuvastatin, enalapril, and enalaprilat in cells and cells + bile was normalized to protein determined using a BCA protein assay (Pierce Chemical, Rockford, IL). The biliary excretion index (BEI; % and in vitro biliary clearance (CL$_{biliary}$; ml/min/kg) were calculated using

B-CLEAR technology (Qualyst Transporter Solutions, LCC, Durham, NC) based on the following equations:

$$\text{BEI} = \frac{\text{Accumulation}_{\text{cells+bile}} - \text{Accumulation}_{\text{cells}}}{\text{Accumulation}_{\text{cells+bile}}}$$

$$\text{CL}_{\text{biliary}} = \frac{\text{Accumulation}_{\text{cells+bile}} - \text{Accumulation}_{\text{cells}}}{\text{AUC}_{\text{medium } 0-T}}$$

where the area under the curve in the medium from time 0 to T ($\text{AUC}_{\text{medium 0-T}}$) represents the product of the incubation time (T) and the initial taurocholate, rosuvastatin, or enalapril concentration in the medium. $\text{CL}_{\text{biliary}}$ units were converted to ml/min/kg body weight based on previously reported values for human protein content in liver tissue (90 mg/g liver weight) and liver weight (25.7 g/kg body weight) (Davies and Morris, 1993).

Sandwich-Cultured Hepatocyte Basolateral Efflux Studies. On day 6 of culture, human SCH were loaded with enalapril for 60 minutes at 37°C with 2 ml/well of standard HBSS containing 5 μM enalapril with and without 25 μM MK-571. The buffer was removed and the cells were washed two times with warm, standard HBSS At this point, 1 ml of methanol containing internal standards was added to one set of each SCH preparation (designated as "pre-efflux SCH") to assess intracellular accumulation of enalapril and derived enalaprilat. Enalaprilat efflux was initiated in the other set of SCH by adding 2 ml of fresh, warm, standard HBSS without enalapril followed by incubation for 30 minutes at 37°C. Aliquots (100 μl) of efflux buffer were taken at 5, 10, and 30 minutes to determine the amount of enalaprilat translocated into the efflux buffer. At 30 minutes, the buffer was aspirated and the cells were washed three times with ice-cold buffer. Post-efflux SCH were lysed in 1 ml of ice-cold methanol containing internal standards. Enalapril and enalaprilat were quantified in efflux buffer, and pre- and post-efflux SCH lysates, by LC-MS/MS (Fig. 1; Table 1). Intracellular enalaprilat concentrations pre- and post-efflux were calculated by dividing the total mass present in the cell lysate by the estimated hepatocyte volume reported previously as 7.69 μl/mg protein,

assuming 1 mg of cellular protein per well (Lee and Brouwer, 2010). Intrinsic basolateral efflux clearance of enalaprilat ($\text{CL}_{\text{int,basolateral}}$) was calculated according to the following equation,

$$\text{CL}_{\text{int,basolateral}} = \frac{X_{\text{Efflux Buffer } t1 \to t2}}{\text{AUC}_{\text{Cell } t1 \to t2}}$$

where $X_{\text{Efflux Buffer}}$ was the cumulative amount of enalaprilat excreted from the cell over the efflux period (t1→t2), assuming that biliary excretion and flux from the bile compartment into the efflux buffer were negligible; AUC_{Cell} represented the log-trapezoidal exposure of intracellular enalaprilat over the efflux period.

LC-MS/MS Analysis. Enalapril and enalaprilat were quantified by LC-MS/MS using an Applied Biosystems (Foster City, CA) API 4000 triple quadrupole mass spectrometer equipped with a TurboV ion source (Applied Biosystems, Foster City, CA), a Shimadzu solvent delivery system (Columbia, MD), and a thermostatted CTC PAL autosampler (Leap Technologies, Carborro, NC). Tuning, operation, integration, and data analysis were carried out in positive mode using multiple reaction monitoring (Analyst software v.1.4.1; Applied Biosystems). Following an 8μl injection onto a Varian Pursuit 3 PFP column (50 × 2 mm, 3 μm particle size; Santa Clara, CA), analytes were eluted via reverse-phase gradient at 0.30 ml/min. Mobile phase A consisted of water and 0.1% formic acid; mobile phase B consisted of methanol with 0.1% formic acid. The initial condition was 80% aqueous, reaching 50% methanol at 1 minute and 97% methanol at 4 minutes. After a 0.4-minute hold at 97% methanol, the mobile phase returned to initial conditions at 4.5 minutes. The total run time, including re-equilibration, was 5 minutes. The specific analytes were monitored as follows: enalapril (377.0 → 234.0), d$_5$-enalapril (internal standard, 382.0 → 239.0), enalaprilat (349.0 → 206.0), and d$_5$-enalaprilat (internal standard, 354.0 → 211.0). Duplicate 8-point calibration curves for both enalapril and enalaprilat (0.075–375 nM) were constructed using the peak area ratio of analyte to deuterated internal standard. In an attempt to mimic the various matrix components (lipids, salts, proteins), separate calibration curves
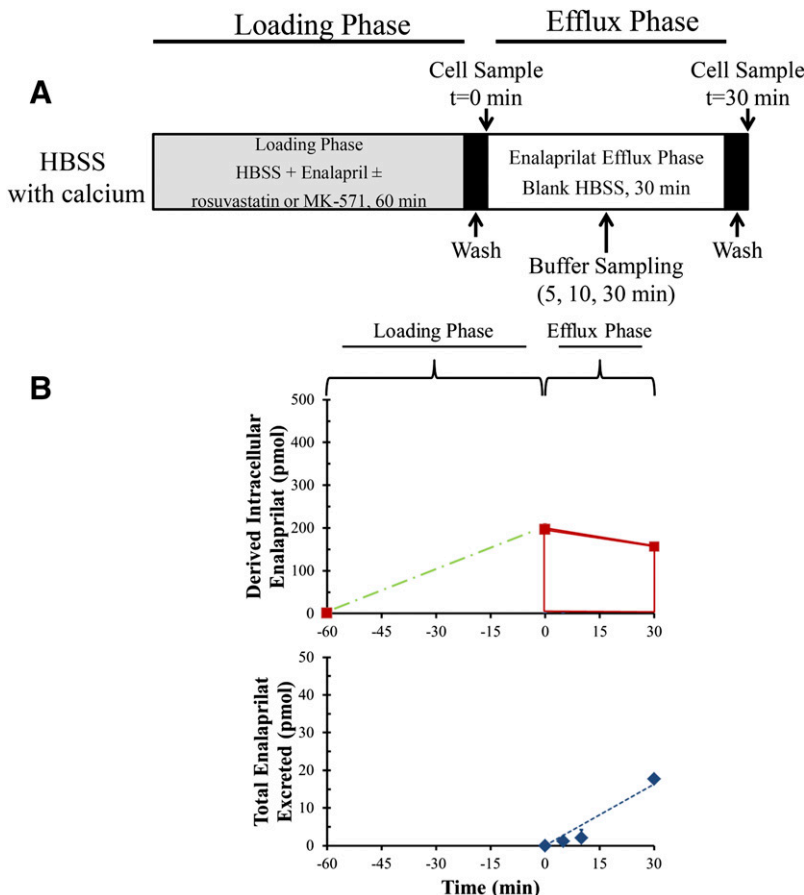

Fig. 1. (A) Scheme depicting efflux studies in human SCH describing the loading and efflux phases (see *Materials and Methods* for a detailed description). (B) Average enalaprilat cellular accumulation (red squares) and mass excreted into the efflux buffer (blue diamonds) observed during the efflux phase in a representative human SCH preparation under control conditions according to the scheme depicted in (A) (mean ± S.D. of triplicate measurements). The green dotted line indicates the presumed cellular accumulation of enalaprilat during the loading phase. Enalaprilat cellular exposure during the efflux phase ($\text{AUC}_{\text{cell } 0 \to 30}$; red trapezoid) was calculated as the log-trapezoidal product of intracellular enalaprilat mass divided by the estimated intracellular volume and time. The mass of enalaprilat excreted into the efflux buffer ($X_{\text{Efflux Buffer}}$) was determined by multiplying the concentration measured in the buffer by the buffer volume.

were constructed with blank matrix from each of the different sample types (i.e., vesicles, cell lysate, and buffer).

Data Analysis. Data are presented as the mean ± S.D. unless otherwise noted. A two-sided Student's *t*-test was used to determine significant differences; in all cases, $P < 0.05$ was considered significant.

Results

ATP-Dependent Transport of Enalapril and Enalaprilat by Membrane Vesicles Prepared from MRP3- and MRP4-Expressing Cells. Prior to enalapril and enalaprilat uptake studies, each batch of membrane vesicles was characterized for protein expression and transport activity of probe substrates as described previously (Köck et al., 2013). ATP-dependent uptake of enalapril and enalaprilat by membrane vesicles prepared from MRP3- and MRP4-expressing cells was determined in vesicles incubated with enalapril or enalaprilat (Fig. 2). ATP-dependent uptake of enalapril was not significantly different in membrane vesicles prepared from MRP3- or MRP4-expressing cells compared with the respective control (Fig. 2A). Although ATP-dependent enalaprilat uptake was not significantly different between control and MRP3-expressing vesicles, statistically significant MRP4-dependent uptake was observed (277 ± 194 pmol/mg protein/min); the uptake rate of enalaprilat was 382 ± 133% greater in vesicles from MRP4-expressing cells compared with mock-transfected control cells. MRP4-mediated enalaprilat transport was investigated in the presence of the prototypical MRP inhibitor MK-571, at a concentration of 50 μM. MK-571 significantly inhibited enalaprilat transport by 83 ± 30% (Fig. 3). MRP4-mediated enalaprilat transport was modestly inhibited by rosuvastatin, but differences were not statistically significant (data not shown).

Human SCH Uptake and Biliary Excretion Studies. Studies were conducted in human SCH to determine the total and cellular accumulation, biliary excretion index, and $CL_{biliary}$ of the positive controls, taurocholate and rosuvastatin. Following a 10-minute incubation of human SCH with 1 μM [³H]taurocholate or 1 μM [³H]rosuvastatin, total accumulation (cells + bile), cellular accumulation (cells), and biliary excretion index (BEI) of taurocholate and rosuvastatin were determined (Fig. 4A). BEI and $CL_{biliary}$ values for taurocholate and rosuvastatin were 81 ± 9% and 22.4 ± 4.6 ml/min/kg body weight, and 39 ± 7% and 6.4 ± 1.3 ml/min/kg body weight, respectively, indicating robust biliary clearance of these compounds (Abe et al., 2009). Additionally, total accumulation, cellular accumulation, and the BEI of enalapril were measured. Following a 10-minute incubation of human SCH with enalapril, a higher total accumulation and cellular accumulation of derived enalaprilat compared with enalapril was observed (Fig. 4B), suggesting rapid and extensive conversion of enalapril to enalaprilat. $CL_{biliary}$ of parent enalapril was negligible in human SCH (0.02 ± 0.01 ml/min/kg body weight; mean ± S.D., $n = 2$ in triplicate). Biliary excretion of derived enalaprilat was not quantifiable in human SCH after a 10-minute incubation period.

Human Sandwich-Cultured Hepatocyte Basolateral Efflux Studies. Basolateral efflux clearance of enalaprilat was assessed in human SCH. Following the 60-minute loading phase with and without MK-571, accumulation of enalapril within the hepatocytes was negligible due to rapid conversion to enalaprilat. Pre-efflux cellular accumulation of derived enalaprilat was decreased when MK-571 was coincubated with enalapril during the loading phase, suggesting inhibition of enalapril uptake processes (Table 1). Correspondingly, with decreased intracellular concentrations over the entire efflux period, the total mass available for efflux across the basolateral membrane in human SCH coincubated with MK-571 also decreased compared with control. Therefore, intrinsic basolateral efflux clearance was calculated by dividing the total mass effluxed across the basolateral membrane by the calculated enalaprilat area under the cellular concentration-time curve (Table 1). MK-571 significantly decreased intrinsic basolateral efflux clearance (Fig. 5; Table 1). Enalaprilat intrinsic basolateral efflux clearance was modestly inhibited by rosuvastatin, but differences were not statistically significant (data not shown).

Discussion

The present study was designed to determine the involvement of MRP3 and/or MRP4 in the basolateral efflux of enalapril and enalaprilat. Using membrane vesicles, MRP3 did not appear to transport either enalapril or enalaprilat. Enalaprilat, but not enalapril, was actively transported by MRP4. To confirm MRP4-mediated transport of enalaprilat, inhibition of uptake by the pan-MRP prototypical inhibitor, MK-571, was evaluated (Köck et al., 2013; Pfeifer et al., 2013b). Indeed, potent inhibition by MK-571 (83%) was observed.

Studies were conducted in human SCH to assess the basolateral efflux of derived enalaprilat in intact hepatocytes. First, the accumulation and biliary excretion of taurocholate and rosuvastatin, two prototypical positive controls that are excreted into bile, were measured to confirm the functionality of the basolateral uptake and canalicular transport processes in the SCH used in this study. Indeed, human SCH exhibited extensive hepatic uptake and biliary clearance of both taurocholate and rosuvastatin. Biliary excretion of enalaprilat was negligible following a 10-minute incubation with enalapril in human SCH (Fig. 4A). Cellular accumulation of preformed enalaprilat in rat SCH was negligible (data not shown), consistent with previously published data demonstrating a diffusional barrier for hepatic uptake of enalaprilat (de Lannoy et al., 1993). Taken together, these data suggest that the basolateral translocation of enalaprilat into the efflux buffer appears to be the only route of excretion of derived enalaprilat in SCH, and that reuptake of enalaprilat does not occur to any measureable extent. Therefore, basolateral excretion of derived enalaprilat was determined in human SCH in the presence and absence of MK-571 to assess the impact of MRP-mediated inhibition of basolateral efflux.
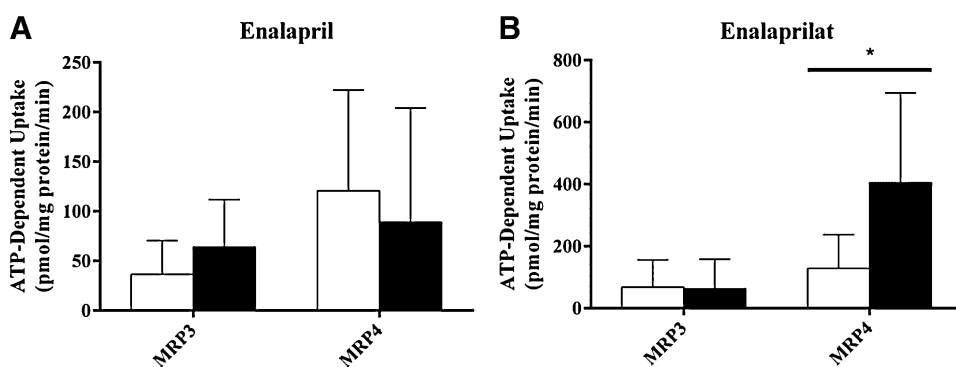
Fig. 2. Transport of enalapril and enalaprilat by MRP3 and MRP4. Uptake of enalapril (100 μM) (A) and enalaprilat (100 μM) (B) into membrane vesicles prepared from HEK293T cells expressing MRP3 or MRP4 (10 μg; solid bars) or mock-transfected controls (10 μg; open bars) was determined after a 5-minute incubation in the presence of ATP or AMP. Data are presented as the mean ± S.D. ATP-dependent uptake into vesicles was determined from three (MRP3) or four (MRP4) independent experiments performed in triplicate; *$P < 0.05$ versus respective control.
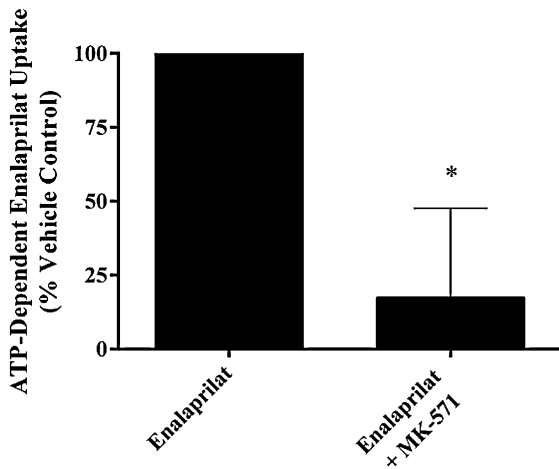
Fig. 3. Effect of MK-571 on MRP4-mediated enalaprilat transport. Membrane vesicles prepared from MRP4-expressing HEK293T cells were incubated with enalaprilat (100 μM) for 5 minutes with and without MK-571 (50 μM). MRP4-dependent, ATP-dependent uptake was calculated and normalized to transport in MRP4 vesicles in the absence of MK-571. Data are presented as the mean $\pm$ S.D. of three independent experiments performed in triplicate; $*P < 0.05$ vehicle control versus MK-571.

[e.g., nonalcoholic steatohepatitis (Hardwick et al., 2011)] would be expected to increase systemic concentrations.

In the present study, a novel basolateral efflux protocol was developed in human SCH to elucidate the impact of basolateral efflux transporter inhibition (e.g., MRP4) on enalaprilat disposition. Following confirmation of the role of MRP4 in enalaprilat transport, basolateral efflux clearance was calculated by dividing the amount of enalaprilat translocated from the hepatocyte into the efflux buffer by the estimated exposure of intracellular enalaprilat. Accurate determination of basolateral efflux using this method assumes that 1) biliary excretion of the compound is negligible; 2) the compound, once effluxed from the hepatocyte, does not re-enter the hepatocyte (i.e., the metabolite must be hepatically derived); and 3) any further conversion from parent to metabolite after the loading phase is insignificant. Data presented in this manuscript suggest that these assumptions are true in the SCH model under the described study conditions. Enalapril and enalaprilat biliary excretion was minimal in human SCH (Fig. 4); thus, potential flux during the efflux phase from the bile canaliculi of SCH into the medium would be negligible. Pilot studies in rat SCH indicated that preformed enalaprilat does not re-enter the hepatocyte (data not shown), consistent with previous reports that enalaprilat is not transported by rat Oatp1a1 (Pang et al., 1998). Although rat Oatp1a1 and human OATP1B1 are not completely homologous, pharmacophore modeling indicated that substrates for these transporters have similar structural moieties (Chang et al., 2005). Finally, the concentration of enalapril in the hepatocyte was very low compared with enalaprilat following both the loading phase and the efflux phase in the human SCH protocol, indicating rapid conversion of enalapril to enalaprilat in the hepatocyte. Alternatively, to assess the impact of delayed conversion of parent to metabolite, the relative concentration of parent to metabolite after the loading phase should be assessed. If the amount of parent left in the cell following the loading phase is greater than 10% of the amount of generated metabolite, conversion during the efflux phase may require further investigation or optimization of the loading protocol. If these assumptions are violated, the interplay between uptake, metabolism, basolateral efflux, and biliary excretion would need to be deconvoluted using mathematical modeling.

Interestingly, the relative extent of inhibition of basolateral efflux clearance of enalaprilat in human SCH was similar to that observed in membrane vesicles prepared from HEK293T cells expressing MRP4 (Figs. 3 and 5); MK-571 inhibition of uptake into membrane vesicles and intrinsic basolateral efflux clearance in human SCH were 83% and 67%, respectively. This finding should be interpreted cautiously because MK-571 is a nonselective MRP inhibitor, and other MRP transporters in addition to MRP4 could contribute to the basolateral efflux of enalaprilat in human hepatocytes.

Following intestinal absorption of enalapril, the predominant route of excretion is presumed to be hepatic metabolism to enalaprilat followed by basolateral efflux of enalaprilat into the systemic circulation and subsequent renal excretion (Ulm, 1983). In isolated perfused rat livers, the magnitude of the basolateral efflux clearance of derived enalaprilat was at least 2-fold greater than biliary clearance (de Lannoy et al., 1993). These preclinical data are consistent with human data indicating that >90% of orally absorbed enalapril is recovered in the urine as enalaprilat (Ulm, 1983). Given this disposition profile, where enalaprilat is excreted preferentially from the liver into the systemic circulation followed by renal excretion, inhibition of MRP4 transport would be expected to decrease systemic enalaprilat concentrations in vivo and the resulting pharmacodynamic effect. The converse also may be true, where increased MRP4 protein expression due to disease

Although inhibition of enalapril uptake would not impact the results of the current study design, it should be noted that enalaprilat cellular concentrations were greatly decreased in human SCH treated concomitantly with MK-571, likely due to inhibition of OATP1B1-mediated uptake of enalapril into hepatocytes. MK-571 is a potent inhibitor (IC$_{50}$ = 0.3 μM) of OATP1B1 (Yamazaki et al., 2005). Importantly, failing to account for decreased uptake by direct measurement of cellular concentrations prior to initiation of the efflux phase may result in overestimation of basolateral efflux inhibition.
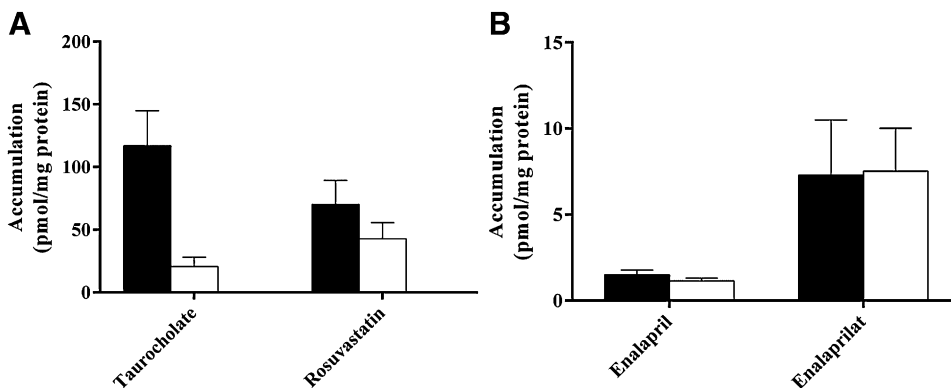

Fig. 4. Disposition of taurocholate and rosuvastatin (A) as well as enalapril and derived enalaprilat (B) in human SCH. Accumulation of taurocholate, rosuvastatin, enalapril, and enalaprilat in cells + bile (black bars) and cells (white bars) in human SCH was measured following a 10-minute incubation with [³H]taurocholate (1 μM), [³H]rosuvastatin (1 μM), or enalapril (5 μM). The BEI was calculated as detailed in *Materials and Methods*; BEI values for enalapril and enalaprilat were negligible. Data represent the mean $\pm$ S.D. of triplicate measurements in three independent hepatocyte preparations for taurocholate and rosuvastatin, or triplicate measurements in two independent hepatocyte preparations for enalapril and enalaprilat.

TABLE 1

Parameters describing hepatically derived enalaprilat disposition in human SCH

Human SCH were incubated with 5 μM enalapril with and without MK-571 (25 μM) for 60 minutes. Enalapril and enalaprilat concentrations in the post-efflux medium, and in hepatocytes pre- and post-efflux, were quantified as described in *Materials and Methods*. Data are presented as the mean $\pm$ S.D.; n = 3 independent hepatocyte preparations performed in triplicate.

Kinetic Parameters	Enalapril (5 μM) Control	Enalapril (5 μM) + MK-571 (25 μM)
Pre-efflux		
Pre-efflux enalaprilat cellular concentration (pmol/μl)		
Liver 1	25.5 $\pm$ 2.5	6.9 $\pm$ 0.6
Liver 2	5.5 $\pm$ 0.3	3.0 $\pm$ 0.1
Liver 3	6.5 $\pm$ 0.7	2.0 $\pm$ 0.2
Mean	12.5 $\pm$ 11.3	4.0 $\pm$ 2.6
Post-efflux		
Post-efflux enalaprilat cellular concentration (pmol/μl)		
Liver 1	20.4 $\pm$ 1.7	5.2 $\pm$ 0.2
Liver 2	5.2 $\pm$ 0.6	3.1 $\pm$ 0.2
Liver 3	6.7 $\pm$ 0.8	2.4 $\pm$ 0.1
Mean	10.8 $\pm$ 8.4	3.6 $\pm$ 1.5
Mass enalaprilat excreted into efflux buffer		
($X_{\text{Efflux Buffer } 0\to30}$, pmol)		
Liver 1	16.9 $\pm$ 1.5	0.8 $\pm$ 1.3
Liver 2	2.3[a]	0.4 $\pm$ 0.7
Liver 3	7.5 $\pm$ 0.6	1.3 $\pm$ 0.5
Mean	8.9 $\pm$ 7.4	0.8 $\pm$ 0.4
Cellular enalaprilat exposure ($\text{AUC}_{\text{Cell } 0\to30}$, pmol·min/$\mu$l)		
Liver 1	684 $\pm$ 16.9	180 $\pm$ 3.2
Liver 2	160 $\pm$ 13.6	91.3 $\pm$ 3.4
Liver 3	199 $\pm$ 16.2	65.4 $\pm$ 4.3
Mean	348 $\pm$ 293	112 $\pm$ 60.4
Basolateral enalaprilat clearance ($\text{CL}_{\text{int, basolateral}}$, μl/min)		
Liver 1	0.024 $\pm$ 0.001	0.004 $\pm$ 0.004
Liver 2	0.014[a]	0.004 $\pm$ 0.007
Liver 3	0.037 $\pm$ 0.002	0.019 $\pm$ 0.008
Mean	0.026 $\pm$ 0.012	0.009 $\pm$ 0.009 *

[a]Value imputed due to analytical error as the difference in enalaprilat intracellular concentration pre- versus post-efflux, assuming a cellular volume of 7.69 μl/mg protein.
*$P < 0.05$ vehicle control versus MK-571.

Results suggest that altered MRP4 function may modulate systemic enalaprilat concentrations and thus enalapril efficacy in vivo. Our group recently identified many drugs as potent MRP4 inhibitors that are commonly coadministered in patients with metabolic disease or hypertension (Köck et al., 2013). In addition to comedications, concomitant genetic variation or disease states may further influence enalapril and enalaprilat pharmacokinetics and pharmacodynamics.
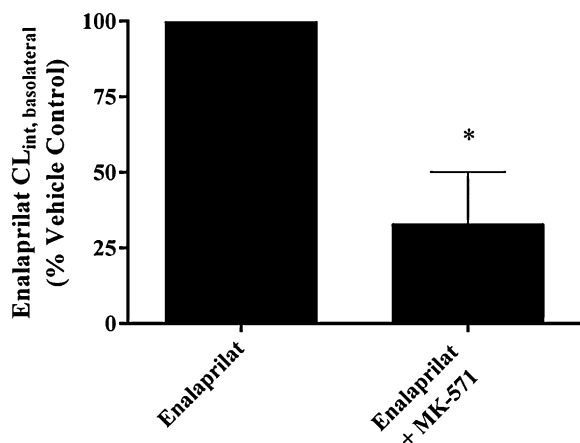
Fig. 5. Effect of MK-571 on the intrinsic basolateral efflux clearance of enalaprilat in human sandwich-cultured hepatocytes. $\text{CL}_{\text{int,basolateral}}$ of enalaprilat was calculated as described in *Materials and Methods*. Clearance values are expressed as a percentage of vehicle-treated control. Data are presented as the mean $\pm$ S.D. of three independent experiments performed in triplicate; *$P < 0.05$ vehicle control versus MK-571.

Interestingly, genetic variation resulting in reduced OATP1B1 function increased enalapril and decreased enalaprilat systemic concentrations, which may lead to decreased systemic pharmacologic activity (Tian et al., 2011). Similarly, patients with inflammatory liver disease (e.g., nonalcoholic steatohepatitis) have decreased OATP and increased MRP4 expression (Fisher et al., 2009; Lake et al., 2011). These changes in transporter expression together with frequent coadministration of potent MRP4 inhibitors [i.e., glyburide, fluoxetine, furosemide, simvastatin (Köck et al., 2013; Morgan et al., 2013)] may unpredictably alter hepatic and systemic concentrations of drugs/ metabolites that are transported in a manner similar to enalapril/ enalaprilat, potentially leading to therapeutic failure or unexpected toxicity. Depending on the culture conditions, MRP4 has been shown to be upregulated in SCH from various species over the culture period (Tchaparian et al., 2011; Noel et al., 2013). Although this does not affect the inhibition profile of MK-571, careful evaluation of factors that alter protein expression in vitro should be considered before data are extrapolated from SCH to in vivo.

Human SCH have been used to mechanistically evaluate hepatocyte vectorial transport and reveal the relative contribution of basolateral versus biliary efflux to overall clearance. Recently, Pfeifer et al. (2013a,b) and Matsunaga et al. (2014) demonstrated the importance of the interplay between basolateral and canalicular efflux in the systemic and hepatic disposition of rosuvastatin and mycophenolic acid glucuronide, respectively. Extensive biliary excretion of rosuvastatin and mycophenolic acid glucuronide required mathematical modeling to deconvolute the contribution of basolateral versus canalicular transport. In contrast, enalapril/enalaprilat exhibited minimal biliary excretion, allowing direct measurement of basolateral efflux in the present

studies. These reports demonstrate that altered hepatic transport may result in modulation of both hepatic and systemic concentrations of drugs and derived metabolites. In fact, inhibition of hepatic uptake and biliary excretion of mycophenolic acid glucuronide, which disrupts enterohepatic recirculation of the parent mycophenolic acid, is postulated as the mechanism behind decreased systemic exposure to mycophenolic acid during coadministration with cyclosporine in transplant patients (Pou et al., 2001; Matsunaga et al., 2014). Additionally, investigation of rosuvastatin disposition in human SCH and isolated perfused rat livers revealed that basolateral and canalicular efflux clearances were approximately equal (Pfeifer et al., 2013a,b). This finding demonstrates that, although rosuvastatin is excreted primarily as unchanged drug in the feces, basolateral efflux in concert with canalicular efflux are key determinants of rosuvastatin overall disposition, and may impact pharmacologic efficacy and/or toxicity. These examples, together with the present study, illustrate the importance of hepatic basolateral and canalicular efflux processes in determining both the pharmacokinetic and pharmaco-/toxicodynamic profile of drugs and their metabolites.

In summary, enalaprilat, the active metabolite of enalapril, is effluxed across the basolateral membrane of hepatocytes by MRP4. MRP4 transport may be inhibited by concomitantly administered drugs (Hasegawa et al., 2007; El-Sheikh et al., 2013; Fukuda et al., 2013). This work highlights the significance of active basolateral efflux in the therapeutic efficacy of active metabolites derived in the liver and excreted into the systemic circulation. SCH represent a robust model to study the interplay between basolateral and canalicular efflux. Further studies are required to understand the mechanistic basis for preferential basolateral or biliary efflux of compounds, and fully appreciate the consequences on the systemic and hepatic action of active/toxic metabolites.

Authorship Contributions

Participated in research design: Ferslew, Brouwer.
Conducted experiments: Ferslew, Köck.
Performed data analysis: Ferslew, Bridges, Brouwer.
Wrote or contributed to the writing of the manuscript: Ferslew, Köck, Bridges, Brouwer.

References

(2011) Enalaprilat for Injection Package Insert Hospira, Inc., Lake Forest, IL 60045 USA, Revised: March 2010.

Abe K, Bridges AS, and Brouwer KLR (2009) Use of sandwich-cultured human hepatocytes to predict biliary clearance of angiotensin II receptor blockers and HMG-CoA reductase inhibitors. *Drug Metab Dispos* 37:447–452.

Chai J, He Y, Cai SY, Jiang Z, Wang H, Li Q, Chen L, Peng Z, He X, and Wu X, et al. (2012) Elevated hepatic multidrug resistance-associated protein 3/ATP-binding cassette subfamily C 3 expression in human obstructive cholestasis is mediated through tumor necrosis factor alpha and c-Jun NH2-terminal kinase/stress-activated protein kinase-signaling pathway. *Hepatology* 55:1485–1494.

Chang C, Pang KS, Swaan PW, and Ekins S (2005) Comparative pharmacophore modeling of organic anion transporting polypeptides: a meta-analysis of rat Oatp1a1 and human OATP1B1. *J Pharmacol Exp Ther* 314:533–541.

Davies B and Morris T (1993) Physiological parameters in laboratory animals and humans. *Pharm Res* 10:1093–1095.

de Lannoy IA, Barker F, 3rd, and Pang KS (1993) Formed and preformed metabolite excretion clearances in liver, a metabolite formation organ: studies on enalapril and enalaprilat in the single-pass and recirculating perfused rat liver. *J Pharmacokinet Biopharm* 21:395–422.

de Lannoy IA and Pang KS (1986) Presence of a diffusional barrier on metabolite kinetics: enalaprilat as a generated versus preformed metabolite. *Drug Metab Dispos* 14:513–520.

El-Sheikh AA, Greupink R, Wortelboer HM, van den Heuvel JJ, Schreurs M, Koenderink JB, Masereeuw R, and Russel FG (2013) Interaction of immunosuppressive drugs with human organic anion transporter (OAT) 1 and OAT3, and multidrug resistance-associated protein (MRP) 2 and MRP4. *Transl Res* 162:398–409.

Fisher CD, Lickteig AJ, Augustine LM, Oude Elferink RP, Besselsen DG, Erickson RP, and Cherrington NJ (2009) Experimental non-alcoholic fatty liver disease results in decreased hepatic uptake transporter expression and function in rats. *Eur J Pharmacol* 613:119–127.

Fukuda Y, Takenaka K, Sparreboom A, Cheepala SB, Wu CP, Ekins S, Ambudkar SV, and Schuetz JD (2013) Human immunodeficiency virus protease inhibitors interact with ATP binding cassette transporter 4/multidrug resistance protein 4: a basis for unanticipated enhanced cytotoxicity. *Mol Pharmacol* 84:361–371.

Ghibellini G, Leslie EM, Pollack GM, and Brouwer KLR (2008) Use of Tc-99m mebrofenin as a clinical probe to assess altered hepatobiliary transport: integration of in vitro, pharmacokinetic modeling, and simulation studies. *Pharm Res* 25:1851–1860.

Gradhand U, Lang T, Schaeffeler E, Glaeser H, Tegude H, Klein K, Fritz P, Jedlitschky G, Kroemer HK, and Bachmakov I, et al. (2008) Variability in human hepatic MRP4 expression: influence of cholestasis and genotype. *Pharmacogenomics J* 8:42–52.

Hanada K, Nakai K, Tanaka H, Suzuki F, Kumada H, Ohno Y, Ozawa S, and Ogata H (2012) Effect of nuclear receptor downregulation on hepatic expression of cytochrome P450 and transporters in chronic hepatitis C in association with fibrosis development. *Drug Metab Pharmacokinet* 27:301–306.

Hardwick RN, Fisher CD, Canet MJ, Scheffer GL, and Cherrington NJ (2011) Variations in ATP-binding cassette transporter regulation during the progression of human nonalcoholic fatty liver disease. *Drug Metab Dispos* 39:2395–2402.

Hasegawa M, Kusuhara H, Adachi M, Schuetz JD, Takeuchi K, and Sugiyama Y (2007) Multidrug resistance-associated protein 4 is involved in the urinary excretion of hydrochlorothiazide and furosemide. *J Am Soc Nephrol* 18:37–45.

Klaassen CD and Aleksunes LM (2010) Xenobiotic, bile acid, and cholesterol transporters: function and regulation. *Pharmacol Rev* 62:1–96.

Köck K and Brouwer KLR (2012) A perspective on efflux transport proteins in the liver. *Clin Pharmacol Ther* 92:599–612.

Köck K, Ferslew BC, Netterberg I, Yang K, Urban TJ, Swaan PW, Stewart PW, and Brouwer KLR (2013) Risk factors for development of cholestatic drug-induced liver injury: inhibition of hepatic basolateral bile acid transporters multidrug resistance-associated proteins 3 and 4. *Drug Metab Dispos* 42:665–674.

König J, Müller F, and Fromm MF (2013) Transporters and drug-drug interactions: important determinants of drug disposition and effects. *Pharmacol Rev* 65:944–966.

Lake AD, Novak P, Fisher CD, Jackson JP, Hardwick RN, Billheimer DD, Klimecki WT, and Cherrington NJ (2011) Analysis of global and absorption, distribution, metabolism, and elimination gene expression in the progressive stages of human nonalcoholic fatty liver disease. *Drug Metab Dispos* 39:1954–1960.

Lee JK and Brouwer KR (2010) Determination of Intracellular Volume of Rat and Human Sandwich-Cultured Hepatocytes (Abstract ID 1595). *The Toxicologist. Supplement to Toxicological Sciences* 114:339.

Liu L, Cui Y, Chung AY, Shitara Y, Sugiyama Y, Keppler D, and Pang KS (2006) Vectorial transport of enalapril by Oatp1a1/Mrp2 and OATP1B1 and OATP1B3/MRP2 in rat and human livers. *J Pharmacol Exp Ther* 318:395–402.

Matsunaga N, Wada S, Nakanishi T, Ikenaga M, Ogawa M, and Tamai I (2014) Mathematical modeling of the in vitro hepatic disposition of mycophenolic acid and its glucuronide in sandwich-cultured human hepatocytes. *Mol Pharm* 11:568–579.

Morgan RE, van Staden CJ, Chen Y, Kalyanaraman N, Kalanzi J, Dunn RT, 2nd, Afshari CA, and Hamadeh HK (2013) A multifactorial approach to hepatobiliary transporter assessment enables improved therapeutic compound development. *Toxicol Sci* 136:216–241.

Noel G, Le Vee M, Moreau A, Stieger B, Parmentier Y, and Fardel O (2013) Functional expression and regulation of drug transporters in monolayer- and sandwich-cultured mouse hepatocytes. *Eur J Pharm Sci* 49:39–50.

Pang KS, Cherry WF, Terrell JA, and Ulm EH (1984) Disposition of enalapril and its diacid metabolite, enalaprilat, in a perfused rat liver preparation. Presence of a diffusional barrier for enalaprilat into hepatocytes. *Drug Metab Dispos* 12:309–313.

Pang KS, Wang PJ, Chung AY, and Wolkoff AW (1998) The modified dipeptide, enalapril, an angiotensin-converting enzyme inhibitor, is transported by the rat liver organic anion transport protein. *Hepatology* 28:1341–1346.

Patchett AA, Harris E, Tristram EW, Wyvratt MJ, Wu MT, Taub D, Peterson ER, Ikeler TJ, ten Broeke J, and Payne LG, et al. (1980) A new class of angiotensin-converting enzyme inhibitors. *Nature* 288:280–283.

Pfeifer ND, Bridges AS, Ferslew BC, Hardwick RN, and Brouwer KLR (2013a) Hepatic basolateral efflux contributes significantly to rosuvastatin disposition II: characterization of hepatic elimination by basolateral, biliary, and metabolic clearance pathways in rat isolated perfused liver. *J Pharmacol Exp Ther* 347:737–745.

Pfeifer ND, Hardwick RN, and Brouwer KLR (2014) Role of hepatic efflux transporters in regulating systemic and hepatocyte exposure to xenobiotics. *Annu Rev Pharmacol Toxicol* 54:509–535.

Pfeifer ND, Yang K, and Brouwer KLR (2013b) Hepatic basolateral efflux contributes significantly to rosuvastatin disposition I: characterization of basolateral versus biliary clearance using a novel protocol in sandwich-cultured hepatocytes. *J Pharmacol Exp Ther* 347:727–736.

Pou L, Brunet M, Cantarell C, Vidal E, Oppenheimer F, Monforte V, Vilardell J, Roman A, Martorell J, and Capdevila L (2001) Mycophenolic acid plasma concentrations: influence of comedication. *Ther Drug Monit* 23:35–38.

Schwab AJ, Barker F, 3rd, Goresky CA, and Pang KS (1990) Transfer of enalaprilat across rat liver cell membranes is barrier limited. *Am J Physiol* 258:G461–G475.

Swift B, Pfeifer ND, and Brouwer KLR (2010) Sandwich-cultured hepatocytes: an in vitro model to evaluate hepatobiliary transporter-based drug interactions and hepatotoxicity. *Drug Metab Rev* 42:446–471.

Tchaparian EH, Houghton JS, Uyeda C, Grillo MP, and Jin L (2011) Effect of culture time on the basal expression levels of drug transporters in sandwich-cultured primary rat hepatocytes. *Drug Metab Dispos* 39:2387–2394.

Tian L, Liu H, Xie S, Jiang J, Han L, Huang Y, and Li Y (2011) Effect of organic anion-transporting polypeptide 1B1 (OATP1B1) polymorphism on the single- and multiple-dose pharmacokinetics of enalapril in healthy Chinese adult men. *Clin Ther* 33:655–663.

Tocco DJ, deLuna FA, Duncan AE, Vassil TC, and Ulm EH (1982) The physiological disposition and metabolism of enalapril maleate in laboratory animals. *Drug Metab Dispos* 10:15–19.

Tsujimoto M, Hatozaki D, Shima D, Yokota H, Furukubo T, Izumi S, Yamakawa T, Minegaki T, and Nishiguchi K (2012) Influence of serum in hemodialysis patients on the expression of

intestinal and hepatic transporters for the excretion of pravastatin. *Ther Apher Dial* **16**: 580–587.

Ulm EH (1983) Enalapril maleate (MK-421), a potent, nonsulfhydryl angiotensin-converting enzyme inhibitor: absorption, disposition, and metabolism in man. *Drug Metab Rev* **14**: 99–110.

Ulm EH, Hichens M, Gomez HJ, Till AE, Hand E, Vassil TC, Biollaz J, Brunner HR, and Schelling JL (1982) Enalapril maleate and a lysine analogue (MK-521): disposition in man. *Br J Clin Pharmacol* **14**:357–362.

Yamazaki M, Li B, Louie SW, Pudvah NT, Stocco R, Wong W, Abramovitz M, Demartis A, Laufer R, and Hochman JH, et al. (2005) Effects of fibrates on human organic anion-transporting polypeptide 1B1-, multidrug resistance protein 2- and P-glycoprotein-mediated transport. *Xenobiotica* **35**:737–753.

Yeung CK, Shen DD, Thummel KE, and Himmelfarb J (2014) Effects of chronic kidney disease and uremia on hepatic drug metabolism and transport. *Kidney Int* **85**:522–528.

Zamek-Gliszczynski MJ, Chu X, Polli JW, Paine MF, and Galetin A (2014) Understanding the transport properties of metabolites: case studies and considerations for drug development. *Drug Metab Dispos* **42**:650–664.

Address correspondence to: Kim L. R. Brouwer, UNC Eshelman School of Pharmacy, University of North Carolina at Chapel Hill, CB #7569, Chapel Hill, NC 27599-7569. E-mail: kbrouwer@email.unc.edu